"HENRI COANDA"
AIR FORCE ACADEMY
ROMANIA

"GENERAL M.R. STEFANIK"
ARMED FORCES ACADEMY
SLOVAK REPUBLIC

INTERNATIONAL CONFERENCE of SCIENTIFIC PAPER
AFASES 2014
Brasov, 22-24 May 2014

THE AERODYNAMIC ANALYSIS OF HIGH LIFT DEVICES

Vasile PRISACARIU[1], Andrei LUCHIAN[2]

[1]Universitatea Transilvania Braşov, [2]Universitatea Politehnica Bucureşti

Abstract: *High lift devices (DHS) are designed to expand the flight envelope by changing the local geometry (mechanization wing), they generally camber changes depending on the phase of flight (landing, take-off). As controls, the aircraft they developed aeromechanical has effects with implications for the resistance structure of the wings, and the most important effect is the twisting of the wing. The article desires a analysis of the 2D aerodynamic profile with changes in curvature at trailing edge.*

Keywords: *high lift devices (HLD), Clark Y, Javafoil 2.20, XFLR5 6.09, Profili 2.21*

1.INTRODUCTION

High lift devices used for bearing surfaces are designed to expand the flight envelope by changing the local geometry (wing mechanization) according to phases of flight of the aircraft. Figure 1.1 is an example of this general concept

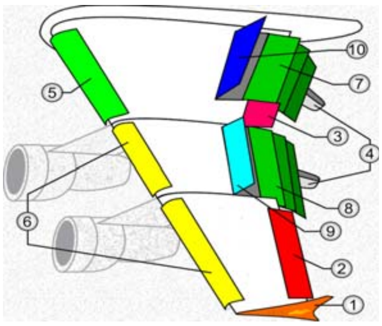

1.winglet, 2.low speed aileron, 3.high speed aileron, 4.flap track fairing, 5.Krüger flaps, 6.slats, 7.three slotted inner flaps, 8.three slotted outer flaps, 9.spoilers, 10.spoilers-air brakes

Fig. 1.1 High lift devices (HLD) [1]

Figure 1.2 presents flaps at Cessna 172.

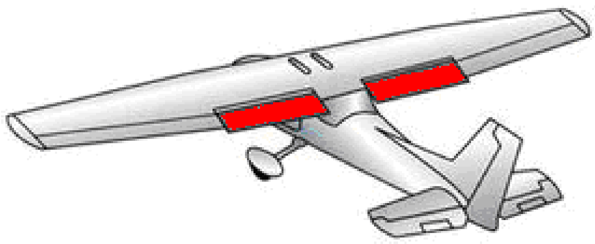

Fig. 1.2 Flaps of Cessna 172,

The use of high lift modern aircraft derived from the need for speed with low values (equation 1) for takeoff and landing phases.

$$V_{at} = \mu_{at} \cdot \sqrt{\frac{2 \cdot G}{\rho \cdot S \cdot c_{z \cdot at}}} \qquad (1)$$

$$F_{z \cdot at} = \frac{\rho \cdot V_{\infty}^2}{2} \cdot S \cdot c_{z \cdot at} \qquad (2)$$

where:

μ_{at} - *factor influencing soil landing, (0.94 – 0.96);*

ρ – *Air density;*

G – Weight of airplane;

S – Lifting surface;

C_{zat} – *lift coefficient in landing configuration*

V_∞ - speed
$F_{z\ at}$ – lifting in landing configuration

In Figure 1.3 the most common types of flaps lifting surfaces.

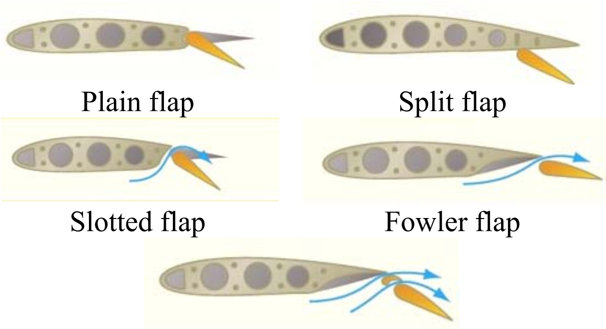

Fig. 1.3 Types of flaps [2, 3]

The methods used to increase the maximum lift coefficient C_{zmax} rely on either modifying the profile geometry (passive systems) or boundary layer control (active systems) or the combination of both methods. High lift studies systems based solely on increasing the bearing surface (type wing folding or telescoping wing), [14]. In carrying devices high lift continuity conditions are imposed to the lifting surfaces produces by the drag increase when high lift is un-prancing and keeping balance during turning to avoid decoupling aerodynamic moments.

Flaps effects

The operation of the wing flaps of curvature increase will cause an increase in lift at the same speed and the ratio T / F_x F_x is changed due to the change value. In this case C_p (pressure center) moves downstream as the steering angle of the flaps increases, thus changing the ratio Fz / G, so it induces a dive time, see figure 1.5.

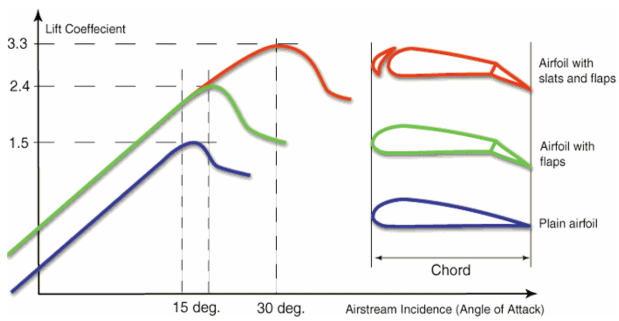

Chart C_z-α

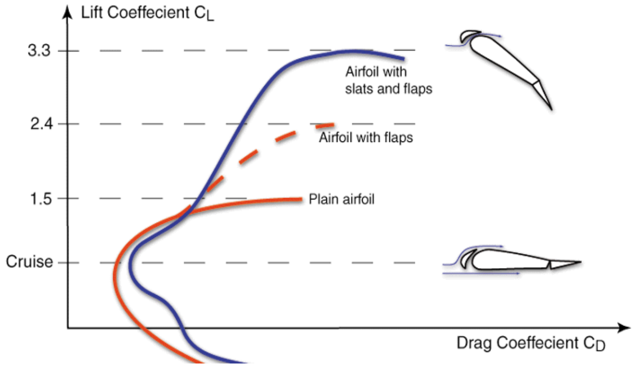

Fig. 1.4 Chart C_z-C_x [4]

When using flaps for negative cycle (up to 50, 100) we have increased cruise by about 5% (transport planes) or better maneuverability for aerobatic maneuvers (aerobatics aircraft).

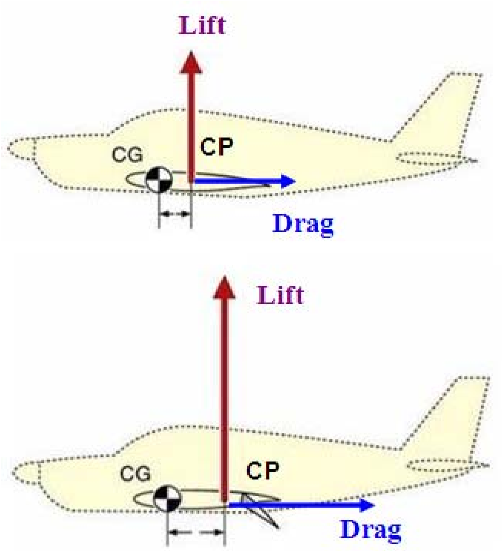

Fig. 1.5 Flaps effects

To increase the effectiveness of flaps we are using some constructive solutions and methods (operational or concept stage):
- Flaps with multiple sections, (Figure 1.6);

Fig. 1.6 Multiple slotted flaps - Boeing 747, [5]

- Spoiler on the upper side in front flaps, figure 1.7;

Fig. 1.7 Spoilers - DC 9, [5]

- slotted flaps rolling extrados surfaces, see figure 1.8, drive / slot Δ_x;

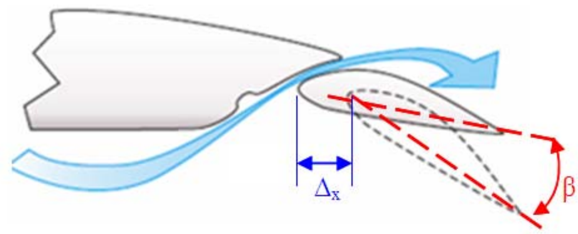

Fig.1.8 Slotted flaps

- blowing boundary layer flow on laminating flap by applying the Coanda effect, the jet flap, [15, 16, 17, 18, 19];

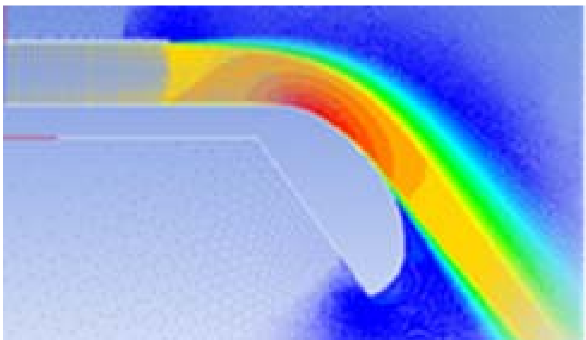

Fig. 1.9 Coandă effect [19]

- Usage of partially morphing to remove pressure jumps in the joints (morphing - no joints, offering a seamless active continuous curvature), or the morphing trailing edge, see figure 1.10, [6, 7, 8];

Fig. 1.10 Morphing concept [6]

- command and control sequences during takeoff / landing fully automated, which eliminates discontinuities maneuver the pilot (autopilot assisted steering gear intervals);
- implementation of the concept "full stall", the landing sequence that leads to a landing speed almost zero;

- flap actuation-correlation with other commands such as thrust vectoring aircraft (aircraft V / STOL), see Figure 1.11.

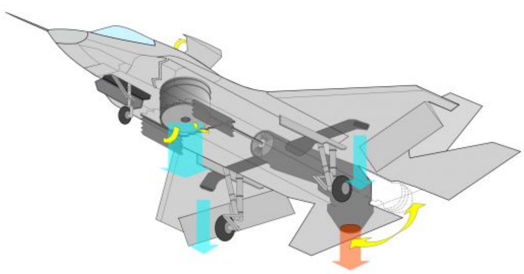

Fig. 1.11 Sukhoi VSTOL (flaps and vectoring traction), [9]

2. THE 2D FLAPS ANALYSIS

We propose to analyze a Clark Y profile with simple flaps with different steering angles, by using four 2D analysis software tools (Javafoil 2.20, Profili 2.20, XFLR5 6.06 and web Airfoil tolls) that are based on Xfoil code. [10, 11, 12, 13].

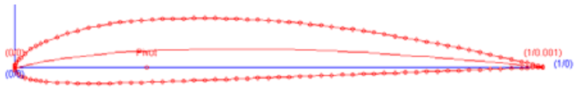

Fig. 2.1 Clark Y airfoil

The study aims to analyze the variation of drag coefficient (Cx, Cz, Cm) depending on the angle of incidence (α), the pressure coefficient (Cp) along the I chord in different positions of the flap deflection. Conditions of the analysis are presented in Table 2.1.

Table 2.1 Conditions of analysis

Definition	121 pct	Viscosity	1,46 x 10^{-5}
Reynolds	100000	Air density	1.221 kg/m^3

2.1. The 2D analysis with flaps 0^0

Viewing the three graphs (Fig. 2.2, 2.3, 2.4) the drag coefficient data depends on the angle of incidence where we can observe the differences in values of the code provided Javafoil and for the three other software environments (profile, XFLR, Xfoil web code) which revealed close values. [11, 12, 13].

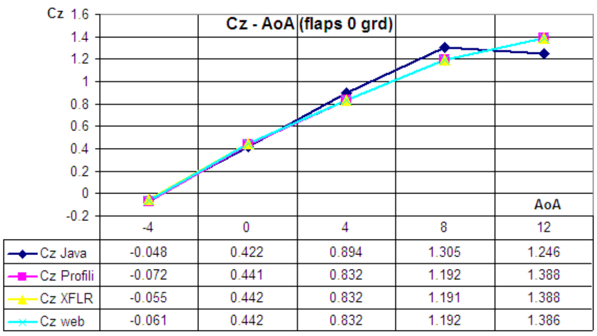

Fig. 2.2 Chart C_z-α (flaps 0^0)

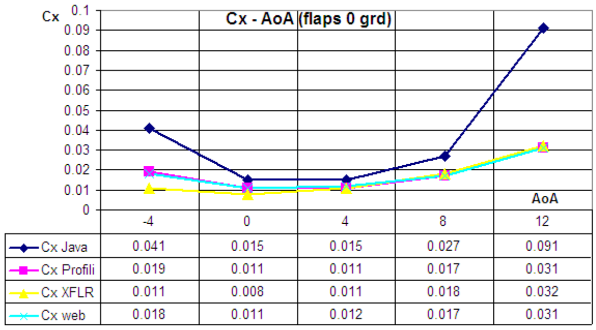

Fig. 2.3 Chart C_x-α (flaps 0^0)

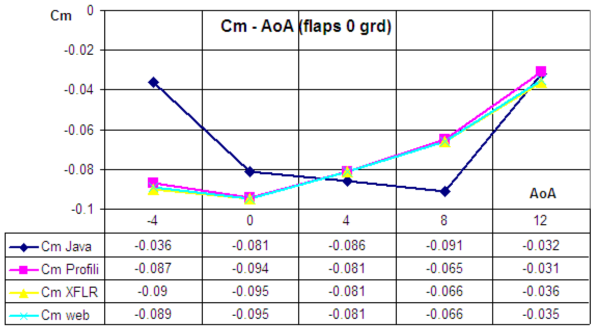

Fig. 2.4 Chart C_m-α (flaps 0^0)

2.2. The 2D analysis with flaps 15^0.

We perform a comparative analysis on 2D flow profile at different angles of deflection with the same software tools.

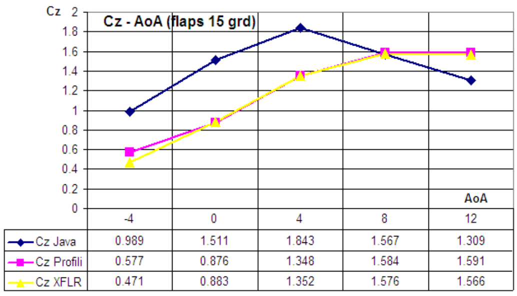

Fig. 2.5 Chart C_z-α (flaps 15^0)

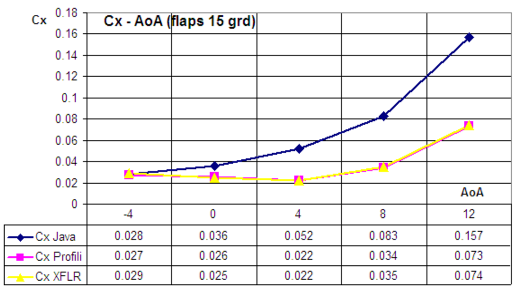

Fig. 2.6 Chart C_x-α (flaps 15^0)

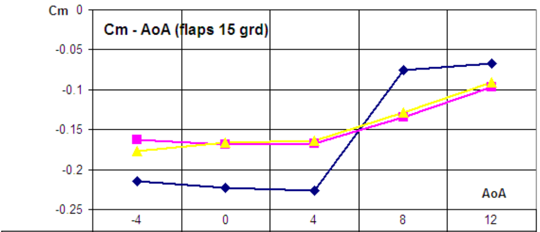

	-4	0	4	8	12
Cm Java	-0.215	-0.223	-0.227	-0.075	-0.067
Cm Profili	-0.163	-0.169	-0.167	-0.135	-0.097
Cm XFLR	-0.177	-0.166	-0.164	-0.129	-0.091

Fig. 2.7 Chart C_m-α (flaps 15^0)

2.3. The 2D analysis with flaps 30^0

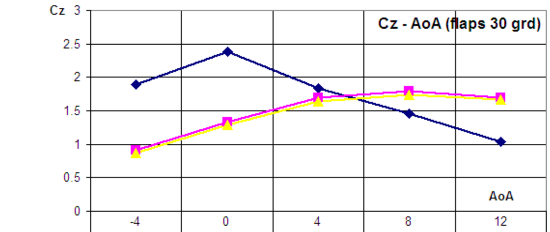

	-4	0	4	8	12
Cz Java	1.887	2.382	1.842	1.464	1.041
Cz Profili	0.912	1.334	1.692	1.798	1.701
Cz XFLR	0.867	1.287	1.643	1.742	1.662

Fig. 2.8 Chart C_z-α (flaps 30^0)

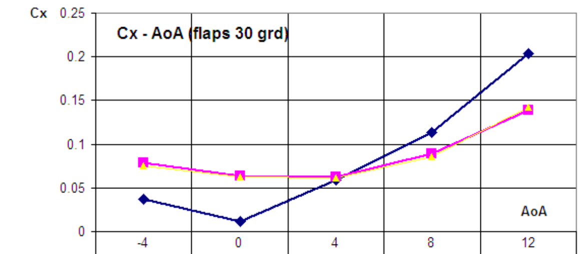

	-4	0	4	8	12
Cx Java	0.037	0.012	0.059	0.114	0.204
Cx Profili	0.079	0.064	0.063	0.089	0.139
Cx XFLR	0.075	0.063	0.061	0.086	0.142

Fig. 2.9 Chart C_x-α (flaps 30^0)

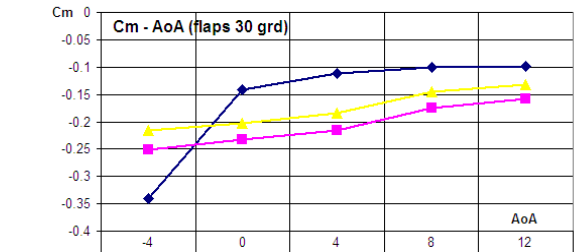

	-4	0	4	8	12
Cm Java	-0.341	-0.141	-0.112	-0.101	-0.098
Cm Profili	-0.252	-0.233	-0.216	-0.174	-0.159
Cm XFLR	-0.216	-0.203	-0.185	-0.146	-0.133

Fig. 2.10 Chart C_m-α (flaps 30^0)

The flap turning effect from 0^0 to 15^0 and 30^0 is illustrated in the graphs in Figures 2.11, 2.12. and 2.13 in the three coefficients compare (Cz, Cx and Cm) using the software environment XFLR5 6.09.

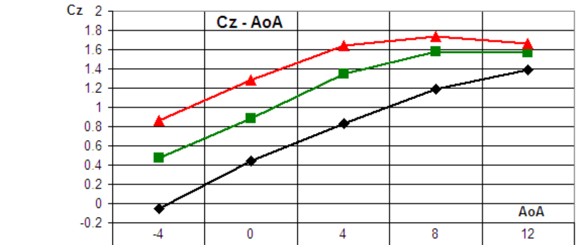

	-4	0	4	8	12
flaps 0 grd	-0.055	0.442	0.832	1.191	1.388
flaps 15 grd	0.471	0.883	1.352	1.576	1.566
flaps 30 grd	0.867	1.287	1.643	1.742	1.662

Fig. 2.11 Chart C_z-α (flaps)

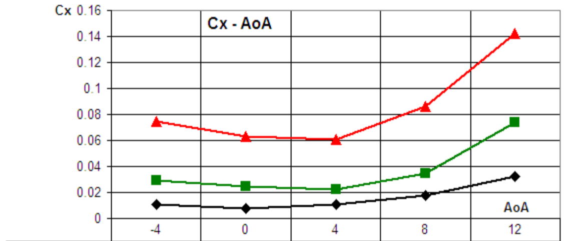

	-4	0	4	8	12
flaps 0 grd	0.011	0.008	0.011	0.018	0.032
flaps 15 grd	0.029	0.025	0.022	0.035	0.074
flaps 30 grd	0.075	0.063	0.061	0.086	0.142

Fig. 2.12 Chart C_x-α (flaps)

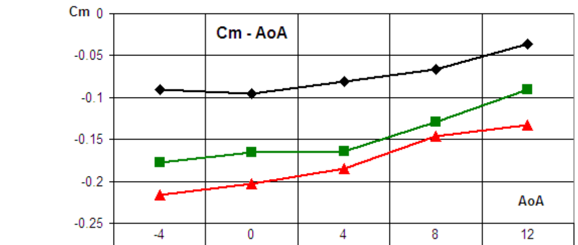

	-4	0	4	8	12
flaps 0 grd	-0.09	-0.095	-0.081	-0.066	-0.036
flaps 15 grd	-0.177	-0.166	-0.164	-0.129	-0.091
flaps 30 grd	-0.216	-0.203	-0.185	-0.146	-0.133

Fig. 2.12 C_m-α (flaps)

The 2D analysis reveals differences in the values provided by the software tools used, but similar numerical developments.

Java foil 2D shows an evaluation tool for highlighting ratio V / V (xfoil code), Figure x shows changes in flow velocity profile

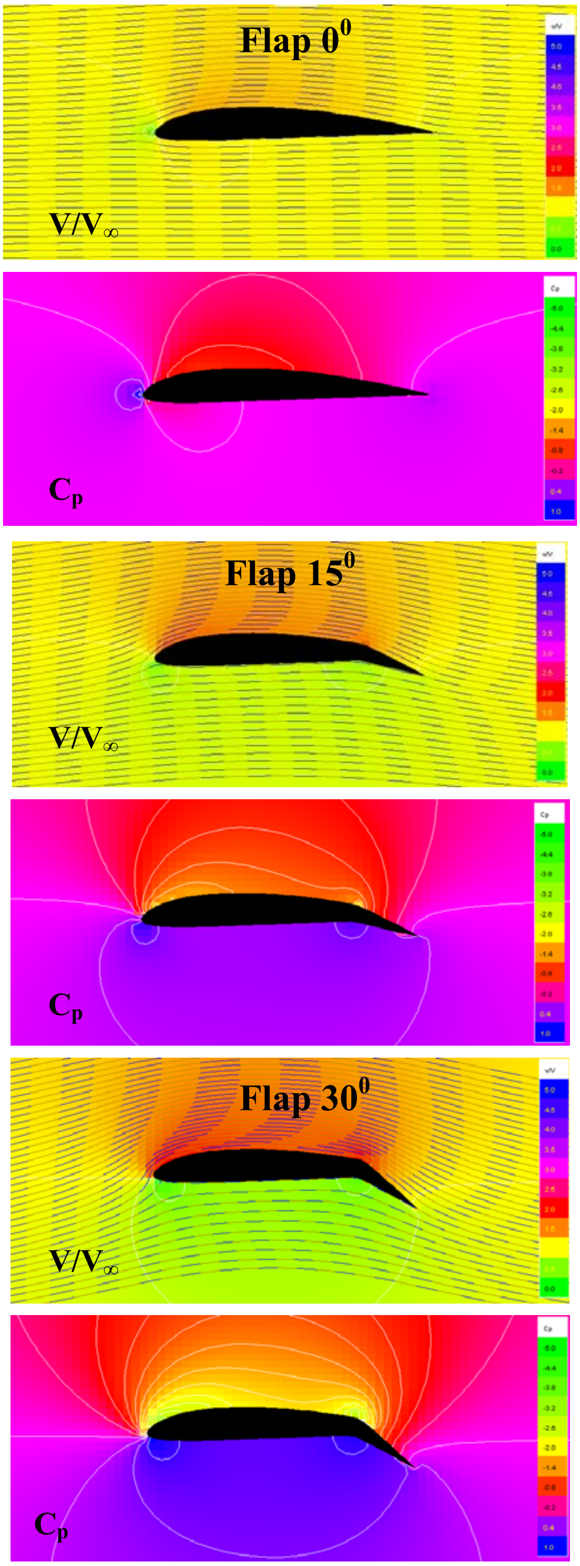

Fig. 2.13 Flow velocity distribution

3. CONCLUSIONS & ACKNOWLEDGMENT

3.1.Conclusions

The main effect of flaps is a generating flow vortex separation on the upper side especially in areas of the surface with air turbulence. Their drive and side effects such as increased dive time decrease the horizontal speed, increasing speed descension, so intervention is required to prevent these effects by correlating flight control (throttle and stick). Aircraft flight control systems Coandă effect can make 3D maneuvers throughout the flight envelope. Next Generation on HDL is morphing concepts combined with smart materials that will increase the efficiency reaction rate of HDL.

3.2. Acknowledgment

The authors wish to thank the "Transilvania" University of Braşov and "Henri Coandă" Air Force Academy of Braşov for supporting the research necessary for writing this article.

BIBLIOGRAFIE

1 http://aviationknowledge.wikidot.com/aviation:wing
2 http://herschlogbook.blogspot.ro/2012/07/aerodynamics-flight-controls.html
3 Young A.D., *The aerodynamic characteristics of flaps*, RAE technical report Aero no. 2622, London, 1953, 56p.
4 http://www.zenithair.com/stolch801/design/design.html,
5 http://www.airliners.net/aviation-forums/tech_ops /read.main/281872/
6 Weisshaar, T.A. (2006) Morphing Aircraft Technology – New Shapes for Aircraft Design. In *Multifunctional Structures / Integration of Sensors and Antennas*. Meeting Proceedings RTO-MP-AVT-141, Neuilly-sur-Seine, France: available at : http ://www.rto.nato.int/abstracts.asp,
7 Prisacariu V., Rău C., Introduction morphing technology in unmanned aircraft vehicles (UAV), AFASES 2011: The 13th International Conference of Scientific Papers "SCIENTIFIC RESEARCH AND EDUCATION IN THE AIR FORCE", mai 2011, Braşov, Romania, , 6p
8 Barbarino S., Bilgen O., and others, *A review of morphing aircraft,* Journal of intelligent material systems and structures, Vol.22/2011, DOI:10.1177/1045389X11414084, p55.

9 http://soni2006.hubpages.com/hub/Thrust-Vectoring-Sukhoi,

10 Hepperle M., JavaFoil 2.20, JAVAFOIL User's Guide, 2014, 44p., disponibil la http://www.mh-aerotools.de/airfoils/javafoil.htm

11 Duranti S. *Profili 2.21 software*, 2012, Feltre-Italia, www.profili2.com, consulted at 12.02.2014

12 Drela M., Yungren H., *Guidelines for XFLR5 v6.03 (Analysis of foils and wings operating at low Reynolds numbers),* 2011, http://sourceforge.net/projects /xflr5/files;

13 Airfoils database, consulted at 10.02.2014, http://airfoiltools.com/airfoil/details?airfoil=clarky-il

14 Mestrinho J.R.C., Felicio J.M.I., and others, *Design optimization of variable-span morphing wing*, 2nd International Conference on Engineering Optimization, September 2010, Lisbon, Portugal, 11p.

15 Williams J., Butler S.F.J., Wood M.N., The aerodynamics of jet flaps, no. 3304, London, 1963, 35p., dsiponibil la http://naca.central.cranfield.ac.uk/

16 Rudolf P.K.C., *High-Lift Systems on Commercial Subsonic Airliners*, NASA contractor report 4746, 1996, 166p

17 Cîrciu I, Dinea S., *Review of application on Coandă effect, history, theories, new trends,* Review of the Air Force Academy, no.2(17)/2010, p14-20, ISSN 1842-9238

18 Cîrciu I., Boşcoianu M., *An analysis of the efficiency of Coandă – NOTAR anti-torque system for small helicopters,* INCAS Bulletin, vol.2, no. 4/2010, ISSN 2066-8201, p.81-88.

19 Dumitrache A., Frunzulica F. , Ionescu T.C., *Mathematical Modelling and Numerical Investigations on the Coanda Effect*, Nonlinearity, Bifurcation and Chaos - Theory and Applications, ISBN 978-953-51-0816-0, http://dx.doi.org/10.5772/50403, , 2012, p101-132,